Aerosol and Air Quality Research, 16: 3037–3054, 2016
Copyright © Taiwan Association for Aerosol Research
ISSN: 1680-8584 print / 2071-1409 online
doi: 10.4209/aaqr.2016.07.0319

Developments in Unipolar Charging of Airborne Particles: Theories, Simulations and Measurements

Chenghang Zheng, Qianyun Chang, Quanyang Lu, Zhengda Yang, Xiang Gao*, Kefa Cen

State Key Laboratory of Clean Energy Utilization, State Environmental Protection Center for Coal-Fired Air Pollution Control, Zhejiang University, Hangzhou, China

ABSTRACT

Charging of airborne particle is an important process in both scientific studies and industrial applications, of which the unipolar charging takes up the major part due to higher charging efficiency. In order to understand the charging mechanism of airborne particles, accordingly to predict the efficiency of unipolar chargers, different theoretical models have been proposed and investigated in all regimes. Numerical techniques have been also adopted by researchers to analyze the charging process of airborne particles and thus to model the unipolar chargers. On the other hand, with the advent and application of various measuring techniques, the electric charges measurement of airborne particles was made possible for researchers. In this work, we mainly present a summary of these models, numerical techniques and experimental results on unipolar charging in all regimes, as well as the recent developments in the design of unipolar chargers, trying to briefly overview the development in this research field.

Keywords: Airborne particle; Unipolar charging; Theoretical models; Numerical simulations; Charger design.

INTRODUCTION

Airborne particles, also known as particulate matter (PM) or particulates, are commonly referred to the particles that are able to suspended in the atmosphere, which can be as respirable suspended particle (RSP; particles with diameter of 10 μm or less), fine particles (diameter of 2.5 μm or less) and ultrafine particles. Airborne particles consist of diverse composition including nitrates, sulfates, elemental and organic carbon, polycyclic aromatic hydrocarbons (PAHs), biological compounds, and metals (Cheruiyot *et al.*, 2015; Kim *et al.*, 2015), which causes severe impacts on climate and human health (Li *et al.*, 2015), fine particles have been extensively studied in diverse fields (Aurela *et al.*, 2015; Malaguti *et al.*, 2015). Among them, the charging process of particles plays an essential part in many applications. For instance, some particle size measurement instruments by electrical differential mobility analysis require the particles to be unipolarly charged with a known charge distribution (Kulkarni *et al.*, 2011), related instruments of which are differential mobility analyzers (DMA) and aerosol particle mass analyzer (APM). Similarly, particle measurement by electrical low-pressure impactors (ELPI) also requires particles to be charged in a corona charger, therefore faradic current produced by charged particles of each channel can be measured (Marjamaki *et al.*, 2000). In addition, particle charging is an important process in gas purification facilities such as electrostatic precipitators (ESPs) (Kim *et al.*, 2012; Qi and Kulkarni, 2012; Liang *et al.*, 2013; Luond and Schlatter, 2013; Clack, 2015) and filtration facilities (Sambudi *et al.*, 2016). Compared with bipolar charging, unipolar charging of airborne particles has attracted particular attention, primarily due to its higher charging efficiency, since the recombination of charged particles with ions of opposite polarity are avoided.

Depending on the mechanisms used to generate gaseous ions for charging, most unipolar chargers can be classified into three types: corona, radioactive, and photoelectric. Corona dischargers are most commonly used to produce high-concentration ions (Hernandez-Sierra *et al.*, 2003; Alguacil and Alonso, 2006; Intra, 2012). The discharging corona is usually produced in a non-uniform electrostatic field, either in a corona-wire or corona-needle configuration. When the field strength is high enough somewhere, ambient air or other gases will undergo an ionization process, and a large amount of gaseous ions and free electrons are generated for charging process. Ionizing radiation is another technique commonly adopted by researchers (Chen and Pui, 1999; Vivas *et al.*, 2008a). Radioactive sources, such as ^{241}Am and ^{210}Po, were used to emit bipolar charged ions, and unipolar ions for charging were separated with an imposed electric field. Photoelectric effect also found its application

* Corresponding author.
Tel.: +86-571-87951335; Fax: +86-571-87951616
E-mail address: xgao1@zju.edu.cn

in airborne particle charging (Han *et al.*, 2003; Hontañón and Kruis, 2008; Kim *et al.*, 2011), when the frequency of the incident radiations, like soft X-ray or ultraviolet (UV) lights, exceed a certain threshold value, electrons can be emitted from the surface of particles, and irradiated particles thus become positively charged. In latest research, soft X-ray chargers are also used in fine particle pre-charging and removal in ESPs (Choi *et al.*, 2016). Recently, new types of chargers such as ion beam aerosol charger (IBAC) (Seto *et al.*, 2003; 2005), surface-discharge microplasma aerosol charger (SMAC) (Kwon *et al.*, 2005; 2007; Manirakiza *et al.*, 2012) and carbon fiber ionizers (Han *et al.*, 2008; Park *et al.*, 2011b) were also introduced as the alternatives of traditional unipolar chargers, with higher charging efficiency for ultrafine particles, controlled ion concentration and less ozone generation, which reduced environmentally hazardous by-products and guaranteed chemical or biological analysis accuracy.

To better describe the unipolar charging process of airborne particles under different circumstances, and more precisely predict and further improve the efficiency of chargers in different applications, numerous charging models have been developed and compared with experimental studies as well. In this article, a summary of typical models and numerical techniques, as well as representative experimental results on unipolar particle charging are presented, aiming to summarize the development of researches concerning the unipolar charging process of airborne particles.

THEORETICAL MODELS ON UNIPOLAR CHARGING

Existing models for unipolar airborne particle charging are primarily classified into three regimes according to their application range (Fig. 1), which is indicated by the Knudsen number (Kn = $2\lambda/d_p$, the ratio of mean free path of gaseous charging ions to the diameter of charged particles). Respectively, the three regimes are continuum regime (Kn << 1), transition regime (Kn ~1) and free-molecular regime (Kn >> 1). This section reviews the progress on theoretical charging model research and compares the theories, hypothesis and application regimes of different models, which are concluded in Table 1.

Continuum Regime

(1) Field Charging

'Field charging' was the first model proposed for particle charging. Based on a rather comprehensive physical view, it was theoretically studied by Pauthenier and Moreau-Hanot (1932). In the model, charged particle is simplified as a conducting sphere suspending in the electric field, and gaseous ions are assumed to be transported to the particle surface along the field lines. As the charging process continues, the particle acquires more electric charges and field lines are gradually repelled from the surface (as shown in Fig. 2).

Under these assumptions, the number of ions deposited on the particle surface is calculated using electrostatic principles. And by integrating the ion current around the particle surface, the overall charging rate in an external electric field E is given by,

$$\frac{dq}{dt} = 3\pi d_p^{\,2} E N_i e Z \left(1 - \frac{q}{q_s}\right)^2 \tag{1}$$

After integration with starting condition t = 0, q = 0:

$$q(t) = q_s \frac{1}{1 + \frac{\tau}{t}} \tag{2}$$

where d_p is the particle diameter, N_i is the concentration of ions above the surface, e the elementary unit of charge, E is electric strength, Z is the electrical mobility of ions, q_s is saturation charge, equals to $(3\varepsilon_s/(\varepsilon_s + 2))\pi\varepsilon_0 d_p^{\,2} E_0$, τ is the time constant of field charging, equals to $4\varepsilon_0/(N_i eZ)$. The formula is applicable for conductive and dielectric particles with different specific dielectric constant.

However, in real cases, the applied electric field is not always uniform, particle charging models in non-uniform fields should be paid attention to. Kim and Yoon (1997) derived a simple expression for the field charging rate of a spherical particle in a linear electric field, while Adamiak (1997) and Samuila *et al.* (1998) studied the charging process of particles in an alternating electric field. Experimental investigations and numerical simulation showed that particles could be charged up to a level close to the saturation value, as

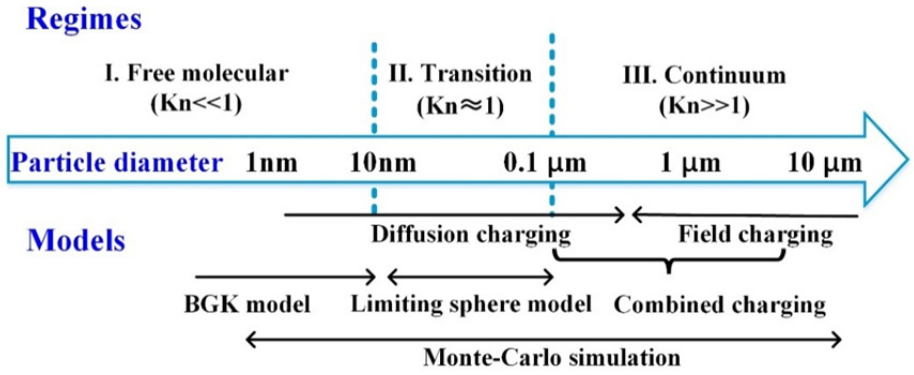

Fig. 1. The scale comparison of charging models.

Table 1. A comparison of theoretical models on unipolar particle charging.

Model	Authors	Interacting forces	Ion velocity distribution	Application regime
Field charging	Pauthenier and Moreau-Hanot (1932)	Coulomb force	n/a	Continuum
Diffusion charging	Fuchs (1947) and Bricard (1949)	Coulomb force	Mean thermal speed	Continuum
Combined charging	Murphy *et al.* (1959), Liu and Yeh (1968), Marlow and Brock (1975) and Lawless (1996)	Coulomb force	Mean thermal speed	Continuum
Limiting sphere	Natanson (1960), Fuchs (1963) and Marquard (2007)	Coulomb and image force	Mean thermal speed	Transition
BGK model	Gentry and Brock (1967), Gentry (1972), Marlow and Brock (1975), Huang *et al.* (1990) and Lushnikov and Kulmala (2005)	Coulomb, image and Van der Waals force (extended later)	Maxwellian	Transition and free molecular
Charge distribution	Boisdron and Brock (1970), Domat *et al.* (2014a)	Coulomb and image force	Mean thermal speed	Transition and free molecular
Non-spherical model	Laframboise and Chang (1977), Chang (1981)	Coulomb force	Mean thermal speed	All
Non-spherical model 2	Gopalakrishnan *et al.* (2013)	Coulomb and image force	Maxwellian	All

predicted by the Pauthenier formula, however, the charging process is not continuous but proceeds only in the time intervals in which the external electric field is stronger than the field produced by the charges already accumulated on the particle. In rest of the time, the resultant electric field repels the ionic bombardment and the particle charge remains unchanged. Lackowski (2001) performed similar numerical calculation, and compared the results with experimental ones, which confirmed the validity of field charging model.

In another aspect, Zevenhoven (1999) analyzed the effect of particle surface conductivity on the unipolar charging process. By allowing for a non-uniform distribution of free charges, the author obtained an expression for the electric current on the particle surface and results showed that a surface charge non-uniformity would lead to a rotation of a particle for a typical field charging case. Similarly, Alisoy *et al.* (2005) investigated the charging of spherical dielectric particles in an electric field, and demonstrated that a stationary particle acquired less charge than a rotating particle. Koseoglu and Alisoy (2011) extended the theory into a stationary and rotational cylindrical dielectric particle in unipolar corona field. Furthermore, Alisoy *et al.* (2010) made the analysis on the effect of particle concentration and mobility on the charging process, and illustrated that the ion density variation and the particle drift velocity could significantly affect the field charging kinetics.

(2) Diffusion and Combined Charging

Although 'field charging' mechanism is generally considered to be predominant for particles with larger than 0.5 μm (White, 1951), it becomes less effective as the particle size decreases. In the cases where low-intensity electric field is applied or smaller particles are adopted, the chaotic motion of gaseous ions thus cannot be ignored. To better describe this charging mechanism of airborne particles, a 'diffusion charging' theory was proposed by Fuchs (1947) and Bricard (1949), respectively. Based on solving the continuum transport equation of ion concentration around a single spherical particle, the ion current in the vicinity of particle surface is calculated by,

$$\frac{\mathrm{dq}}{\mathrm{dt}} = \frac{2\pi D_i d_p \mathrm{N_i}}{\int_1^\infty \left(\frac{1}{x^2}\right) exp\left[\frac{e^2}{4\pi\varepsilon_0 d_p kT}\left(\frac{q}{x} - \frac{\varepsilon_s - 1}{\varepsilon_s + 1}\frac{e}{2x^2\left(x^2-1\right)}\right)\right] dx} \tag{3}$$

where D_i is ionic diffusion coefficient (equals to Z(k/e)T), d_p is the particle diameter, N_i is the ion concentration, e the elementary unit of charge, x is the ration of r and a, r is distance from the center of the particle, a is the radius of the particle, ε_0 is the vacuum dielectric constant, ε_s is the dielectric constant of particle.

White (1951) later derived a simpler expression for diffusion charging from gas kinetics theory, which was later pointed out to be also valid in free molecular regime (Gentry and Brock, 1967; Liu *et al.*, 1967b). The diffusion charge is expressed by,

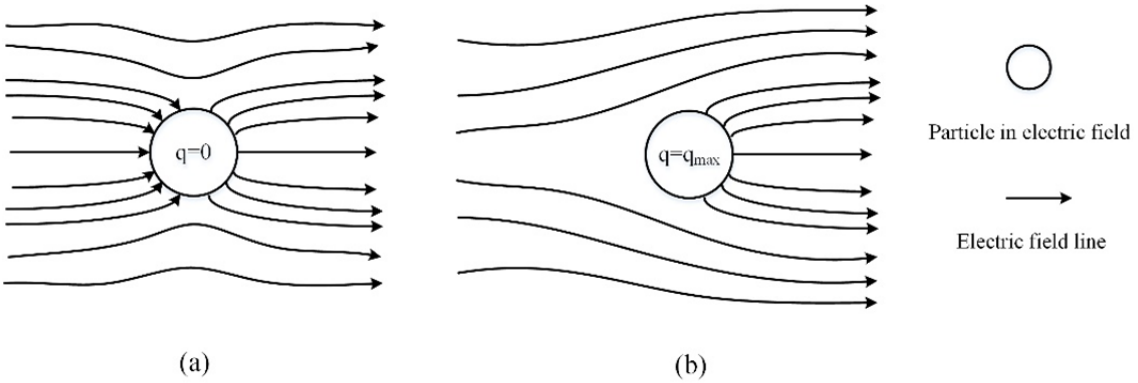

Fig. 2. Electric field line around a particle (a) an uncharged particle (b) a particle with saturation charge.

$$q(t) = q^* \ln\left(1 + \frac{t}{\tau^*}\right) \tag{4}$$

$$q^* = \frac{2\pi\varepsilon_0 d_p kT}{e} \tag{5}$$

$$\tau^* = 8\varepsilon_0 \left(\frac{m_i kT}{3}\right)^{\frac{1}{2}} \left(\frac{ZE}{d_p Je}\right) \tag{6}$$

where t is time, q^* is particle charge constant, τ^* is the time constant of diffusion charging, d_p is the particle diameter, N_i is the ion concentration, e the elementary unit of charge, ε_0 is the vacuum dielectric constant, m_i is ion mass, Z is the ion mobility, k is the Boltzmann constant and J is current density.

Thus, to take both charging mechanisms into account, researchers have made different approaches to combine these two models in a reasonable way. Murphy (1959) made the first trial but ended up only in qualitative analysis. Another method was taken by Liu and Ye (1968) who divided the entire charging process into two time steps. Before reaching the saturation charge limit, the particle is subject to both charging mechanisms, while after that, it is only 'diffusion charging' that works. Similar but more complex model was obtained by Smith and McDonald (1975), who identified three regions on the particle surface, and calculated the overall charging rate as the sum of them. Till now, a most commonly used model was developed by Lawless (1996), which has been extensively used in the numerical simulations of electrostatic precipitators (Long and Yao, 2012; Guo *et al.*, 2013; Lancereau *et al.*, 2013). The charging rate is expressed in a dimensionless form as:

$$\frac{dv}{d\tau} = \begin{cases} f(w)\dfrac{v-3w}{\exp(v-3w)-1}, & v > 3w \\ \dfrac{3w}{4}\left(1-\dfrac{v}{3w}\right)^2 + f(w), & -3w \le v \le 3w \\ -v + f(w)\dfrac{-v-3w}{\exp(-v-3w)-1}, & v < -3w \end{cases} \tag{7}$$

where f(w) is the fraction of surface covered by diffusion band,

$$f(\mathrm{w}) = \begin{cases} \dfrac{1}{(w+0.475)^{0.575}}, & w \ge 0.525 \\ 1, & w < 0.525 \end{cases} \tag{8}$$

where $v = qe/2\pi\varepsilon_0 d_p kT$ is the dimensionless particle charge, $w = (\varepsilon_s/\varepsilon_s + 2)(Ed_p e/2kT)$ is the dimensionless electric field strength, and $t = (\rho_s b_i t/\varepsilon_0)$ is the dimensionless charging time.

Transition and Free Molecular Regime

(1) Limiting Sphere Model

In the non-continuum regime, where the diameter of particles is in the same magnitude or even smaller than the mean free-path of gaseous ions, the image force induced by the charged particle cannot be ignored. Therefore, previous charging models for airborne particles in continuum regime no longer fit here.

The charging model in transition regime was first proposed by Natanson (1960), and later developed by Fuchs (1963) as the 'limiting sphere' model. It assumes that the particle charging region is separated by an imaginary sphere concentric to the particle. Inside the sphere, the ions are supposed to travel without collisions with gas molecules (shown in Fig. 3), so the number of ions striking the particle in unit of time is given by:

$$\mathrm{I} = 4\pi\delta^2 n(\delta)\frac{\bar{c}}{4}\alpha \tag{9}$$

$$\delta = \frac{{d_p}^3}{\lambda^2}\left[\frac{\left(1+\dfrac{\lambda}{d_p}\right)^5}{5} - \frac{\left(1+\dfrac{\lambda^2}{{d_p}^2}\right)\left(1+\dfrac{\lambda}{d_p}\right)^3}{3} + \frac{2}{15}\left(1+\frac{\lambda^2}{{d_p}^2}\right)^{\frac{5}{2}}\right] \tag{10}$$

where δ is the limiting-sphere radius, n(δ) ion concentration on the limiting sphere, $\bar{c}$ the mean thermal velocity of the ions, and α the fraction of all the emerging ions which finally reaches the particle surface.

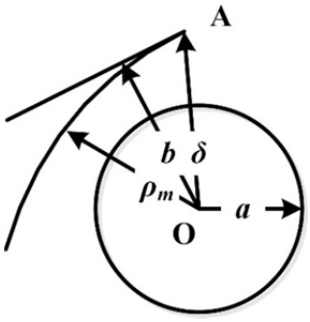

Fig. 3. Motion of ions inside the limiting sphere (Fuchs, 1963).

Natanson (1960) calculated the overall probability α of the collision between ions and the airborne particle, given by:

$$\alpha = (b_m/\delta)^2 \tag{11}$$

$$b^2 = \rho_m{}^2 \left\{1+\frac{2}{3kT}\left[\varphi(\delta)-\varphi(\rho_m)\right]\right\} \tag{12}$$

where $\varphi(\rho)$ is the potential of the ion, b distance from O to the tangent drawn to the trajectory at point A, and b_m the minimum value of b. Outside the sphere, the charging process is described by the classic diffusion theory of ions. To match the two fluxes at the surface of the limiting-sphere, the charging rate of a single particle is derived.

Marquad (2007) extended the model into a 2D form to include the presence of external electric field. As a result of imposed electric field force, the collision probability α is no longer constant for ions striking from different angle, but turned out to be a function of azimuthal angle, expressed as α(θ). Similarly, the electrostatic potential map around the limiting sphere is recomputed with the existence of external electric field, and continuum convective-diffusion equation is solved for the ion concentration profile on the limiting sphere at different angle. In this way, by integrating the ion current around the limiting sphere surface, the overall ion current is obtained according to,

$$\beta_i = \frac{I}{eN_{i,\infty}} = \int_0^{\pi} 2\pi\delta^2\overline{c}\,\frac{N_i(\delta,q,\theta)}{N_{i,\infty}}\alpha(q,\theta)\,\mathrm{d}\theta \tag{13}$$

where β_i equals to $I/(eN_{i,\infty})$, integral combination coefficient. I is the current through the limiting sphere. where q is the particle charge, n_∞ the ion concentration at infinity, and thus extended the limiting sphere theory into a more elaborate 2D model with wider application in the transition regime.

(2) Boltzmann Equation and BGK Model

Nevertheless, due to the mean velocity assumption employed in the limiting sphere model, it will probably underestimate the acquired charge of finer particles under certain conditions. Gentry and Brock (1967) took a different approach, trying to illustrate the unipolar charging mechanism with a first order approximation of Boltzmann equation.

Since the ion concentration is sufficiently low that ion-ion interactions can be neglected, the gas system can be described by the Boltzmann equation. The equations for the ions i and neutral gas j have the following forms,

$$\frac{\partial f_i}{\partial \mathrm{t}} + v_i \cdot \frac{\partial f_i}{\partial \mathrm{X}} + F_i \cdot \frac{\partial f_i}{\partial v_i} = \Gamma_i\left(f_i f_j\right) \tag{14}$$

$$\frac{\partial f_j}{\partial \mathrm{t}} + v_j \cdot \frac{\partial f_j}{\partial \mathrm{X}} = \Gamma_j\left(f_j f_j\right) \tag{15}$$

where f_i and f_j are the velocity distribution functions of ions and neutral gas molecules in the neighborhood of the particle, X is the spacial vector, v_i and v_j represent velocity vectors of ions and neutral gas molecules, Γ_i and Γ_j are the appropriate collision operators, and F_i is the force vector per unit mass acting on an ion owing to the presence of charge on the particle.

The net flux of ions to a particle is determined from the moments of the velocity distribution functions of ions striking and reflecting from the particle surface respectively. A rather complicated expression is found for the net radial flux of ions to a conducting particle. Later, Gentry (1972), Marlow and Brock (1975) modified the theory, and took the image force into account, while Huang (1990) took Van der Waals force into consideration as well. More recently, Lushnikov (2005) further developed the BGK model in the free molecular regime. Based on a solution of the collisionless kinetic equation about ion transport in the presence of force fields created by the particle charge and the image force, they used the exact free-molecule ion distribution over coordinates and velocities to calculate the rate of ion deposition onto neutral and charged dielectric particles, which is applicable for particles with the size much smaller than the ion mean free path.

(3) Charge Distribution Model

Previous descriptions of the unipolar charging processes for airborne particles were largely averaged or deterministic in nature, whereas, Boisdron and Brock (1970) pointed out that such descriptions are inadequate for charging process.

Apparently, collision of an ion or radioactive atom with a particle is a random event, thus resulted a statistical distribution of ions on the poly-disperse particles or even mono-disperse ones. Combining Natanson's (1960) expressions on the ion fluxes with the Boltzmann-like equations of the concentrations of the particles, the equations can be re-written in the expanded form:

$$\begin{aligned}
\frac{\mathrm{d}N_{p,0}}{\mathrm{dt}} &= -\beta_0 N_{p,0} N_i \\
\frac{\mathrm{d}N_{p,1}}{\mathrm{dt}} &= \beta_0 N_{p,0} N_i - \beta_1 N_{p,1} N_i \\
&\vdots \\
\frac{\mathrm{d}N_{p,n}}{\mathrm{dt}} &= \beta_{n-1} N_{p,n-1} N_i - \beta_n N_{p,n} N_i
\end{aligned} \tag{16}$$

where $N_{p,n}$ is the concentration of airborne particles with n elementary charges, N_i is the ion concentration, and β_n is the combination coefficient of ions with airborne particles carrying n elementary charges. Together with the initial boundary conditions, the steady-state charge distribution on airborne particle clusters is determined.

However, this set of equations neglects both ion and particle losses and supposes that ions and particles are uniformly mixed in the charging region. Recently, a revised charging model based on the birth-and-death theory was developed. In the work of Kimoto *et al.* (2010), they estimated the effect of electrostatic dispersion on particle losses in the charging chamber with the assumption that particles are completely mixed with unipolar ions in the charging chamber and compared the calculated results with experimental results. Furthermore, Domat *et al.* (2014a) proposed a revised model including both diffusional and electrical losses for airborne particles and ions. The electrical loss is modeled with the inclusion of a radial electric field which is considered constant throughout the charging region, while the diffusional one is expressed by a loss factor determined from the ratio between the total volume occupied by the ions and the surface area where they are probably loss. In this way, this model can be used to more precisely predict the charge distribution in real unipolar chargers, as well as to obtain the ion concentration and mean radial electric field from the measured charge distribution fractions, without additional measurements.

Non-Spherical Particle Charging Model

Despite the varieties of charging models for airborne particles mentioned above, none of them is applicable to non-spherical particles. A charging model towards arbitrarily shaped particles was first developed by Laframboise and Chang (1977). The model also assumes that the charge transport to the particle is governed by the continuum transport equation and ions have a sticking probability per collision with the particle surface. Chang (1981) re-examined the theory and provided simpler equations depending on the Kn_{ion}. The mean charge of airborne particle obtained from unipolar diffusion charging is governed by the following equations:

In continuum regime ($Kn_{ion} \to 0$),

$$n_p \cong C_p N_i Dt / \varepsilon_0 \left(\phi_p < 0.1\right) \cong \frac{2C_p kT}{e^2}\left[\left(\frac{e^2}{kT}\frac{N_i Dt}{\varepsilon_0}+1\right)^{0.5}-1\right]\left(\phi_p < 1\right) \quad (17)$$

and in free molecular regime ($Kn_{ion} \to \infty$),

$$n_p = \frac{2C_p kT}{e^2}\ln\left(1+\frac{e^2\bar{c}}{4kT}\frac{N_i S_p t}{C_p}\right) \quad (18)$$

where n_p is the mean charge of airborne particle, C_p is the electrical capacitance, ϕ_p is the non-dimensional surface potential $eV_p/(kT)$, V_p is the electric potential of a particle relative to the potential at large distance, S_p is the geometric surface area of particle.

Most recently, Gopalakrishnan (2013) applied a different method, trying to describe the charging process with collision kernel based equations. The charging rate for airborne particles with p number of charges is calculated as:

$$R_{p,i} = \beta_{p,i} N_p N_i \quad (19)$$

where N_p and N_i are the airborne particle and ion number concentrations, and $\beta_{p;i}$ is the collision rate coefficient or kernel of ions and particle. To obtain the collision kernel for airborne particles with arbitrary shape, Gopalakrishnan utilized a dimensional analysis method to identify different shapes with two dimensionless number: the Coulomb potential energy ratio, and the image potential energy ratio. With the examination of molecular dynamics (MD) and Brownian dynamics (BD) calculations, an expression for collision kernel was found applicable for particles of any shape. The simulation results also indicated that this model could provide more accurate predictions in the transient regime than the limiting sphere model.

Numerical Techniques on Unipolar Charging Process

(1) Monte-Carlo Simulation

Despite the comprehensive physical pictures embedded in those models above, few of them are able to capture the charging characteristic of particles with complex shapes. In an effort to describe the charging process of such airborne particles, a Monte-Carlo code has been developed by Filippov (1993), and was later developed and extended to wider applications by Biskos (2004).

The Monte-Carlo method is well-known and widely used in modeling and describing transport phenomenon, by using large numbers of realizations to compile the average behavior. As illustrated in Fig. 4, the simulation volume consisted of uniformly distributed particles and ions that move randomly according to their thermal velocities. Since the particles are significantly more massive compared to ions, they are considered to be fixed in the simulation volume. In the simulation process, as is mentioned before, the ions are assumed to move in straight paths between ion-particle collisions far off the charged particles. But when an ion gets close enough to a charged particle, the velocity is significantly altered by the ion-particle interaction force, and the speed distribution departs from Maxwellian. Solving the dynamic equation of ions numerically along the free path accordingly results in the ion trajectories near the particle. After large numbers of iterations, the averaged charge acquired is determined. For agglomerates, the total charge number is the sum of that on every elementary particle.

Filippov (1993) developed the first Monte-Carlo simulation code on unipolar charging process, and particles with diameters between 5 and 80 nm were adopted in the calculation. The calculation results were compared with previous experimental data of Adachi *et al.* and other researchers (Adachi *et al.*, 1985; Romay and Pui, 1992), as well as the predictions of limiting sphere model. As is shown in Fig. 5, Monte-Carlo method and the limiting sphere model gave relatively close results, which agreed fairly well

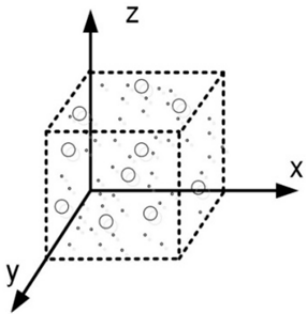

Fig. 4. Schematic representation of the Monte-Carlo simulation volume (Biskos *et al.*, 2004).

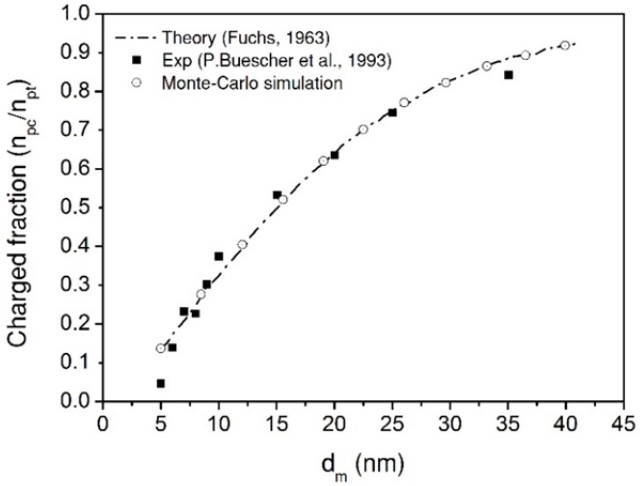

Fig. 5. Simulation results and comparisons by Filippov (1993).

with experiments in the entire diameter range. Likewise, Biskos (2004) also examined the Monte-Carlo method for particles in the size range of 5 to 1000 nm, and further extended it into non-spherical particles charging, where rectangular shape particles, chain aggregates and 3D cross-shape aggregates were employed. A close agreement was found between Monte-Carlo method and the charging models for spherical particles. As for non-spherical airborne particles, however, the charging behavior exhibited significant divergence compared with theoretical predictions, which calls on further studies on this topic.

(2) Numerical Modelling of Unipolar Chargers

Apart from the Monte-Carlo simulations on theoretical charging processes, researchers also developed numerical techniques to analyze the charging process in unipolar chargers. Aliat *et al.* (2008; 2009) presented a two-dimensional numerical model on airborne particle charging in a negative wire-tube corona charger with the combination coefficients of negative ions and electrons to airborne particles calculated by Fuchs's model, the numerical results of which showed good agreement with experimental data of Marquard (2005). Alisoy (2012) also developed a numerical method to investigate the charging kinetics of poly-disperse particles in a coaxial electrode system, where a previous charging model considering ion concentration and particle mobility was adopted (Alisoy *et al.*, 2010). Alonso (2009) investigated and compared the effects of four different initial mixing state on the charging process, which is often ignored by other researchers.

Besides, particle and ion loss to the walls by diffusion and electrostatic dispersion were also taken into account in the calculations (Alonso and Alguacil, 2003, 2007). Numerical results show that the charger's extrinsic charging efficiency (the percentage of neutral particles which acquire charges in the conditioner and make the exit of charger) strongly depends on the initial mixing state, and the maximum efficiency is achieved when a core of ions is surrounded by airborne particles, a state which has been in practice by injecting ions and particles into the charger through two coaxial cylinders. Kimoto *et al.* (2010) compared the experimental results with the calculations results and the results showed that particle loss caused by electrostatic dispersion was reduced by use of the small volume charging chamber.

Towards the practical application of numerical techniques, Chien *et al.* (2011, 2013) developed a two-dimensional (2D) numerical model to predict the charging process in real unipolar chargers with complex geometries, which contains the fully coupled calculation of flow field, electric potential and ion concentration fields, and the charging dynamics of airborne particles. Methods for calculating the fields is based on the work of Lin and Tsai *et al.* (2010), while the charging model developed by Marlow and Brock (1975) was adopted to calculate the particle charging efficiency, and good agreement between the predicted and experimental charging efficiencies was obtained. The numerical results also showed the advantage of using sheath air on minimizing the charged particle loss, which is accordingly able to facilitate the design of unipolar chargers for airborne particles.

In addition, Huang and Alonso (2011, 2012) investigated the trajectories and charging dynamics of particles and electrostatic loss within a corona needle charger by solving the governing equations on flow field, electric field, and particle motion. Simulation results showed that the number of charges acquired per particle depends on the parameters of particle diameter, radial position from the symmetry axis, applied voltage, Reynolds number, and axial distance along the charger. A similar 2D numerical model on a corona needle charger was also developed and evaluated by Park *et al.* (2011a). However, some of researchers employed the charging models only in continuum regime, which may cause some error towards the modelling of nanoparticle charging.

Finally, to evaluate different charging models, Long and Yao (2010) used a numerical model of the electrostatic precipitator and nine particle charging models including field charging theory, diffusion charging theory and combined field-diffusion theory were compared against experimental data based on the particle charge, particle motion and particle collection efficiency. The results showed that prediction results of the constant charging models were better than that of the non-constant models but differed little for the sub-micrometer particles and a first choice of model was given for numerical models of the particle dynamics in electrostatic precipitators

Comparison of Experiments with Theoretical Models

With the advent and application of various measuring techniques, the electric charge measurement of airborne particles was made possible for researchers. To examine the accuracy and applicability of particle charging models, numbers of experiments on unipolar charging of particles have been conducted by researchers. In this section, we present a brief summary of the relevant work, which is concluded in Table 2.

(1) Continuum Regime

Pauthenier and Moreau-Hanot (1932) performed one of the first measurements on particle charging of continuum regime. In the experiment, metallic and insulating spheres with diameter ranging from 10 to about 200 μm were released in a negative corona field. By analyzing the trajectories of particles, the charges on each particle were obtained and results showed the agreement with the 'field charging' model. Different from case of solid spheres adopted above, Fuchs *et al.* (1936) measured the acquired charge of oil-droplets ranging from 0.5 to 3 μm in radius, and good agreement was also obtained between averaged measured charges and theoretical predictions by 'field charging' model for all sizes of droplets studied (Fig. 6).

More elaborate measurement was conducted by Hewitt (1957) using a cylindrical mobility analyzer, and he took a charge-mass-ratio method as a comparison. He obtained convincing data on the charging process of particles with diameters ranging from 0.07 and 0.66 μm, which was later verified to agree with the combined field and diffusion charging model by Liu and Kapadia (1978). Regarding the diffusion charging of particles, Liu *et al.* (1967a) examined the model at low pressures with a cylindrical mobility analyzer, and a reasonable agreement was found between the experimental data and the formula derived by White. Similarly, Kirsch and Zagnit'Ko (1981, 1990) also conducted several experiments to verify the diffusion charging model in the presence of a weak electric field and vapors of different liquids, and results showed that the acquired charges of di-2-ethylhexyl sebacate (DES) and dibutyl phthalate (DBP) particles with radius between 0.05 and 1.5 μm agree fairly well with Fuchs's diffusion charging theory.

Towards the examination of combined charging models, McDonald *et al.* (1980) performed an experiment in the continuum regime using Millikan cell. Experimental results showed agreement with the combined charging model by Smith and McDonald (1975) for positive corona while indicating a certain variance for negative corona at higher temperature, which was possibly attributed to the 'free electron charging mechanism'. Frank *et al.* (2004) measured the electric charges on droplet particles of 0.1–20 μm in diameter with three different methods, and results showed that the average charge agreed fairly well with the prediction of combined charging model by Lawless (1996). Most recently, Long and Yao (2010) summarized different kinds of charging models in continuum regime and reexamined them with the experimental data of Hewitt (1957), which indicated that Lawless model should be the first choice relatively for modelling particle charging dynamics in electrostatic precipitators.

(2) Transition and Free Molecular Regime

In non-continuum regime, measurement on the airborne particle charging was first performed by Adachi *et al.* (1985) using zinc chloride ($ZnCl_2$) and di-2-ethyl hexyl sebacate (DEHS) particles of 4–100 nm in diameter. Mono-disperse particles were obtained at the exit of differential mobility analyzer (DMA), and then get charged by unipolar ions produced by α ray from Am-241. Results showed that the charged fraction of particles was in quite good agreement with the prediction of limiting sphere model.

Pui *et al.* (1988) also examined the unipolar charging models in non-continuum regime. Mono-disperse, uncharged silver (Ag) and sodium chloride (NaCl) particles with diameter ranging from 4 to 75 nm were exposed to unipolar ions produced by a corona discharge. The results (Fig. 7) indicated that the BGK model by Marlow and Brock (1975) best predicted the combination coefficient in the entire size range, while above 10 nm, the data approached the limiting sphere model, which was consistent with Adachi's experiment above.

Apart from those concerns on charged fraction, Biskos *et al.* (2005) employed a TDMA system to investigate the mean charges and actual charge distributions on airborne particles in transition regime. Mono-disperse particles with diameter between 10–300 nm were adopted, while the measurements showed fairly good agreement with limiting sphere theory and the charge distribution model. Similarly, Alguacil and Alonso (2006) also measured the charge distribution on airborne particles in diameter below 35 nm, by employing tandem differential mobility analyzer (TDMA) setup. The average charges per particle predicted by limiting sphere theory was in relatively good agreement with the experimental results despite the existence of high intensity electric field in the charging region.

Besides, Oh *et al.* (2004) studied non-spherical particle charging experimentally for the first time. TiO_2 agglomerates were produced by thermal decomposition of titanium tetraisopropoxide (TTIP) vapor, charged by the indirect photoelectric charger and the average charge of particles was measured by particle electrometer and condensation particle counter. Experimental results showed that aggregates with a low fractal dimension have about 30% more charges than spherical particles since particles with a lower fractal dimension have larger surface area and self-capacitance. Shin *et al.* (2010) further studied the effect of particle morphology on unipolar diffusion charging of particle agglomerates, and found that the experimental data was in good agreement with estimates of Chang's theory.

In respect of other factors in particle charging process, Shin *et al.* (2009) investigated the material dependence of the charging process experimentally. The examined particles (10–200 nm) covered a wide range of dielectric constant with almost the same spherical or compact morphology. Measurements of both charged fraction and mean charge per particle showed very small differences among different materials. And the level of the small difference was consistent with the estimation by limiting sphere model. Qi *et al.*

Table 2. Experimental results and comparison on unipolar particle charging.

Continuum regime						
Researchers	Method	Temperature	Pressure	Material	Diameter range	Verified model
Pauthenier and Moreau-Hanot (1932)	Trajectory analysis	Room temperature	1 atm	Metal and insulating spheres	10–200 μm	Field charging
Fuchs *et al.* (1936)	Oscillation method	Room temperature	1 atm	Oil droplet	1–6 μm	Field charging
Penney and Lynch (1957)	Parallel mobility analyzer	Room temperature	1 atm	DOP	0.3–0.6 μm	Field charging
Hewitt (1957)	Cylindrical mobility analyzer	Room temperature	1 atm	DOP	0.07–0.66 μm	Combined charging
Liu *et al.* (1967)	Cylindrical mobility analyzer	Room temperature	0.031–0.96 atm	DOP	0.65 and 1.35 μm	Diffusion charging
McDonald *et al.* (1980)	Millikan cell	37–343°C	1 atm	DOP	0.6–3 μm	Combined charging
Kirsch and Zagnit'Ko (1981)	Oscillation method	Room temperature	1 atm	DES and DBP	0.06–2 μm	Diffusion charging
Kirsch and Zagnit'Ko (1990)	Oscillation method	Room temperature	1 atm	DES and DBP	0.1–3 μm	Field and diffusion charging
Frank *et al.* (2004)	DMA	Room temperature	1 atm	DOP and glycerol	0.1–20 μm	Combined charging
Non-continuum regime						
Researchers	Method	Temperature	Pressure	Material	Diameter range	Verified model
Adachi *et al.* (1985)	DMA	Room temperature	1 atm	$ZnCl_2$ and DEHS	4–100 nm	Limiting sphere and charge distribution
Pui *et al.* (1988)	Electrical particle analyzer	Room temperature	1 atm	NaCl and Ag	4–75 nm	Limiting sphere and BGK model
Oh *et al.* (2004)	DMA	Room temperature	1 atm	TiO_2 agglomerates	50–200 nm (mobility diameter)	Non-spherical model
Biskos *et al.* (2005)	TDMA	Room temperature	0.25–1 bar	combustion particle	10–300 nm	Limiting sphere and charge distribution
Alguacil and Alonso (2006)	TDMA	Room temperature	1 atm	Ag	5–35 nm	Limiting sphere and charge distribution
Qi *et al.* (2009)	DMA	Room temperature	1 atm	Ag, NaCl and sucrose	10–200 nm	Limiting sphere
Qi *et al.* (2009)	DMA	Room temperature	1 atm	NaCl	50–200 nm	Limiting sphere and charge distribution
Shin *et al.* (2010)	DMA	Room temperature	1 atm	Silver sphere and agglomerates	30–200 nm (mobility diameter)	Limiting sphere and non-spherical model

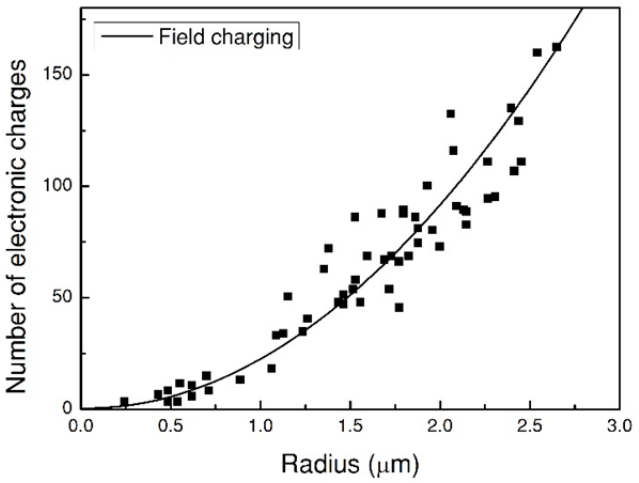

Fig. 6. Experimental results and comparison by Fuchs (1936).

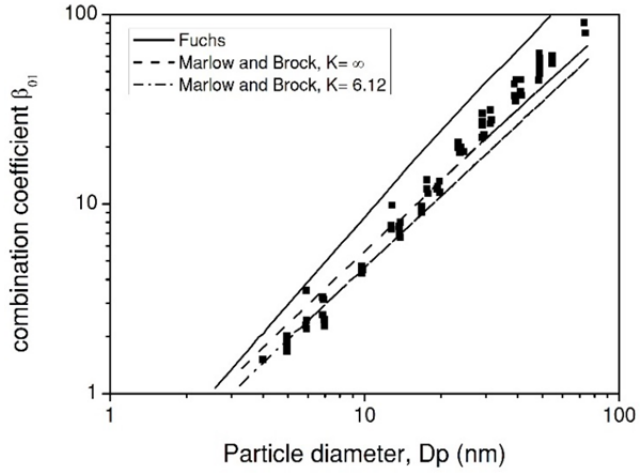

Fig. 7. Experimental results and comparisons by Pui *et al.* (1988)

(2009) investigated the effect of particle pre-existing charges on unipolar charging, and particles in diameter between 50 and 200 nm carrying a certain number and polarity of pre-existing charges were employed in the experiment. The results from the analytical solution of limiting sphere and charge distribution model showed very good agreements with experimental data regarding the relationship between the preexisting charge and the final charge on particles.

Recent Progresses in Unipolar Charger Design

In addition to the above-mentioned proving charging experiments, in practical applications, however, the charging efficiency is the most important index evaluating the performance of unipolar charger. In order to achieve higher charging efficiency and less electrostatic loss with nano-sized particle charging, researchers have been dedicated in promoting new designs of unipolar chargers for years. Another key a parameter to describe the operation effect of unipolar charger is the N_it product, i.e., the multiplication of mean ion number concentration and particle residence time. To improve particle charge, the N_it product should be enlarged. Therefore improvement of ion concentration and residence time is necessary for improving particle charge. However, as for a practical charger, particle loss due to electrostatic dispersion and particle diffusion. What's more, both negative and positive discharging can be used in unipolar dischargers. However, ozone can be generated as a common by-product in negative discharging while positive discharging won't have the problem. Positive discharging is used in areas such as particle measurement instruments (ELPI) and air cleaner while negative discharging is widely used in industry facilities such as ESPs.

Intra and Tippayawong (2009, 2011) reviewed the historical development of unipolar chargers. In this session, we will mainly focus on the most recently developed unipolar chargers, and respective applicable charging models. The ion properties used in the calculation of unipolar chargers designs are concluded in Table 3 and comparison of parameters in different unipolar particle chargers is shown in Table 4.

Han *et al.* (2008) developed a novel kind of unipolar charger using carbon fiber ionizers, which consisted of a bundle of approximately 300 carbon fibers with the diameter of about 5–10 μm. In the experiment, a positive DC voltage of 2.3–4.0 kV was applied to the carbon fiber ionizers, and as shown in Fig. 8, an extrinsic charging efficiency of about 60% was achieved for 20 nm particles at 2.3 kV, showing good agreement with calculated the intrinsic charging efficiency based on limiting sphere charging theory with ion properties from previous studies (Han *et al.*, 2003).

In another study, a corona-discharge based, unipolar mini-charger was developed by Qi *et al.* (2008), which is only 25 mm in length and 12.5 mm in diameter, consisting of an outer metallic case and a pointed tungsten needle electrode as the discharge module. Despite of its compact size, it has demonstrated good intrinsic and extrinsic charging efficiencies for particles ranging from the submicron (higher than 80%) down to 5 nm (about 60%) in a low flow rate (0.3 L min^{-1}). Whereas, higher extrinsic charging efficiency was achieved in a high flow rate of 1.5 L min^{-1} since lower particle losses in the charging zone. However, the agreement between the experimental and calculated charge distributions was not satisfactory, which may be attributed to the non-uniform distribution of ion concentration and electrical field.

Tsai *et al.* (2010) developed a unipolar charger containing multiple gold discharging wires in a tube, and investigated the charging performance of nano-sized particles. By shortening the residence time in the charging region, the optimal extrinsic charging efficiency was obtained and the charger's extrinsic charging efficiency increased from 2.86% to 86.3% in the charger as the particle diameter increasing from 2.5 to 50 nm. Moreover, particle charge distribution at the exit was analyzed using TDMA system, and results showed that most particles are singly charged or uncharged for diameter smaller than 10 nm while the fraction of multiply charged particles becomes higher for particles larger than 20 nm.

Additionally, Vivas *et al.* (2008b) reported their effort on optimizing an existing diffusion charger developed by Büscher *et al.* (1994) to reduce the multiple charging of submicron airborne particles. By imposing an ion-driving

Table 3. Ion properties used in the calculation of unipolar chargers designs.

Researchers	Polarity	Mobility	Mass	Diffusion coefficient	Reference
Han *et al.* (2008)	+	1.1	130	2.78	Shimada *et al.* (2002)
Qi *et al.* (2008)	+	1.15	290	3.0	Reischl *et al.* (1996)
Tsai *et al.* (2010)	+	1.40	n/a	n/a	n/a
Vivas *et al.* (2008)	+	1.40	109	3.54	Adachi *et al.* (1985)
Park *et al.* (2009)	+	n/a	n/a	n/a	n/a
Kimoto *et al.* (2010)	+ / -	1.40 / 1.90	130 / 50	3.54 / 4.9	Mohnen (1976)
Li and Chen (2011a)	+	1.40	109	3.57	Pui *et al.* (1988)

Table 4. Comparison of parameters in different unipolar particle chargers.

Researchers	Ion source	Sheath air	Applied Voltage	$N_i t$ (s cm^{-3})	Extrinsic charging efficiency
Kwon *et al.* (2007)	Surface microplasma	No	n/a	$3.0–3.9 \times 10^{12}$	3.0% at 3.4 nm (+) 4.2% at 3.4 nm (−)
Qi *et al.* (2007)	Corona	No	n/a	$5.4–9.0 \times 10^{6}$	6.1 at 4 nm (+)
Han *et al.* (2008)	Carbon fiber ionizer	No	+2.3–4 kV	$4.4–9.6 \times 10^{12}$	60% at 20 nm (+)
Qi *et al.* (2008)	Corona	No	n/a	n/a	19–80% at 10–50 nm (+)
Tsai *et al.* (2008)	Corona	Yes	+4–10 kV	2.72×10^{8}–3.87×10^{9}	10.6–74.2% at 10–50 nm (+)
Vivas *et al.* (2008)	Corona	No	+4.5 kV	8×10^{10}–6×10^{12}	19–63% at 50–250 nm (+)
Park *et al.* (2009)	Corona	No	+3.5–5 kV	$1–6 \times 10^{6}$	n/a
Kimoto *et al.* (2010)	Corona	Yes	+4–9 kV and –4–9 kV	1.31×10^{8} and 1.56×10^{8}	59–71% (+) and 46–66% (–) at 5–40 nm
Tsai *et al.* (2010)	Corona	Yes	+4–10 kV	n/a	2.86–86.3% at 2.5–50 nm (+)
Li and Chen (2011b)	Corona	No	+200–600 V and –200–600 V	5.0×10^{6}–1.2×10^{7}	7.29–88.3% at 5–50 nm (+)
Li and Chen (2011a)	UV charger	No	n/a	n/a	38.9–87.8% at 7–30 nm
Domat *et al.* (2014b)	Corona	No	+2.0–4.5 kV	n/a	24.9–81.5% at 9–40 nm (+)
Alonso and Huang (2015)	Corona	No	+2.8–3.5 kV	n/a	4–48% at 4–10 nm (+)

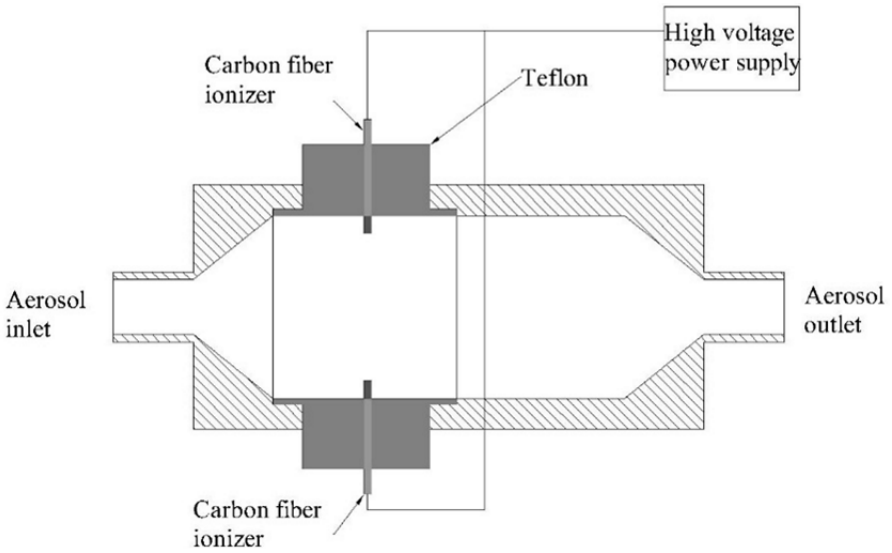

Fig. 8. Schematic diagram of the unipolar charger developed by Han *et al.* (2008).

voltage on the grid between the ion-generation and charging chambers, as well as minimizing the grid length and duty cycle of imposed voltage, the multiple charging of the particles of 250 nm was greatly reduced. For a flow rate of 1.5 L min^{-1}, the extrinsic charging efficiencies of 19% and 63% are attained with the corona charger for particles of, respectively, 50 and 250 nm. Comparison between the analytical solution given by Biskos *et al.* (2005) and

experimental extrinsic efficiency showed reasonably good agreement.

Park *et al.* (2009) designed a new type of diffusion charger for determining the geometric standard deviation of particle sizes as well as the geometric mean diameter and the total number concentration of particles, which consisting of discharge zone, mixing and charging zone, three flow channels, and ion trap zone. we introduce a methodology. In this work, the estimated $N_i t$ product for 3.5 to 5 kV of applied voltage was within $1–6 \times 10^6$ s cm^{-3}, and the particle losses were below 12% for particle in all channels. The author also evaluated the average charge and charged fraction of particles in three different channels based on TDMA system, and results showed that the calculation based on charge distribution model acquired good agreement with the experimental data.

Moreover, as shown in Fig. 9, a small mixing-type unipolar charger (SMUC) for airborne particles was developed by Kimoto *et al.* (2010). The charger has a small charging chamber of only 0.5 cm^3 volume to reduce particle loss caused by electrostatic dispersion, and the High-Pressure Corona (HPC) ionizer described by Adachi *et al.* (2004) and Whitby (1961) was used as a unipolar ion generator. The average charging time was 0.025 s when the flow rates of ions and particle were 0.2 and 1 L min^{-1}, and the optimum discharge conditions were achieved when the applied voltage is +8 or –9 kV. Under such conditions, the measured extrinsic charging efficiencies are 0.46–0.66 and 0.59–0.71 for negative and positive charging, respectively, in the particle size range of 5–40 nm. Since the negative ion mobility in air in higher than that of positive ions, resulting in higher ion loss due to electrostatic dispersion and particle diffusion, therefore the extrinsic charging efficiency of positive corona discharge is higher than that of negative discharge. Measurement results also showed that the experimental charging efficiencies agree well with the results calculated without considering electrostatic dispersion, suggesting that particle loss due to electrostatic dispersion is reduced by the use of small-volume charging chamber.

Li and Chen (2011b) also designed a DC-corona based charger (Fig. 10), consisting of a tungsten needle as discharging electrode, and a cylindrical grounded metal case. The charging experiment was conducted at a flow rate of 3 L min^{-1} and an ion-driving voltage of 600 V. It is reported the extrinsic charging efficiency is higher than 60% for particles of diameters larger than 15 nm. The birth-and-death charging model was used to obtain the calculated charge distributions of particles, and reasonable agreement was achieved when compared with the measured charge distributions. The authors (2011a) also investigated the charging performance of an particle charger based on pen-type UV-lamps ,which was a quartz tube about 7 inches long surrounded by four low pressure Hg lamps with a 6 inches lighted length. Results showed the extrinsic charging efficiency of the charger was higher than 80% for particles of diameters larger than 15 nm, and a comparatively good agreement was also obtained between the experimental and calculated charge distributions in the study.

Besides, Domat *et al.* (2014b) investigated the effect of electrode gap on the performance of a corona charger with separated corona and charging zones. Similarly, the ion chamber is concentric to the outer casing and surrounded by the particle flow, which was shown in a theoretical study (Alonso *et al.*, 2009) to be the best configuration for unipolar diffusion chargers. Due to its flexible design on the gap between electrode and outer casing, the charger is able to vary the onset voltage and ion concentration over a wide range, therefore the intrinsic and extrinsic charging efficiencies and charged particles loss. Experimental results indicated that varying the electrode gap distance is an efficient way to regulate the ion concentration, as well as the charging performance.

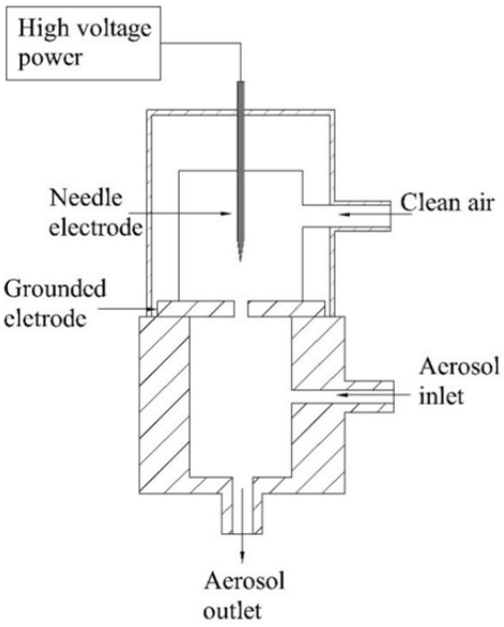

Fig. 9. Schematic diagram of the small mixing-type unipolar charger developed by Kimoto (2010).

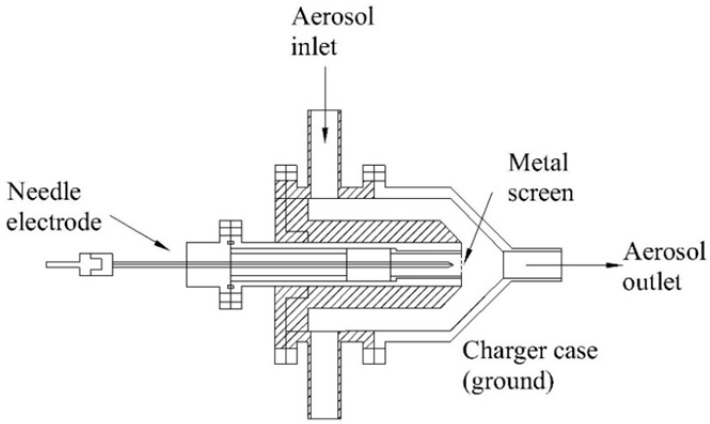

Fig. 10. Schematic diagram of the DC-corona based charger developed by Li and Chen (2011b).

Most recently, Alonso and Huang (2015) designed an electrical charger based on a point-to-plate DC corona discharge for particle charging below 10 nm. diameter below 10 nm. In spite of its simple design, the specific design allowed relatively small diffusion and electrostatic losses since the small effective charging volume in comparison with other typical designs. As a consequence, the extrinsic charging efficiency attainable was higher than published similar devices of Chen and Pui (1999), Tsai *et al.* (2010), Chien *et al.* (2011), etc. for particle size in the range 5–10 nm while for smaller particles the charging efficiencies was slightly lower than those attainable chargers with sheath air to reduce particle diffusion losses.

SUMMARY AND FUTURE WORK PROSPECT

Unipolar charging is one of the most important techniques applied in airborne particle studies in laboratories and industrial applications. In this work, a historical development of theoretical models and numerical methods of unipolar particle charging are reviewed, and relevant experimental results are summarized and compared with theoretical ones.

In the continuum regime, the field/diffusion charging models act as primeval models with only limited application range, while combined charging models may yield quite satisfying predictions universally. However, in the non-continuum regime, when the particle size approaches the mean free path of gas molecules, charging models become more detailed and require much more precise description on the charging process. Limiting sphere and BGK model both provide applicable solutions in non-continuum regime within certain range. Moreover, charging models towards the charge distribution and non-spherical particles have been also proposed and verified by researchers.

As the development of theoretical models, the numerical techniques in modelling the particle charging process are also advancing in recent years. The Monte-Carlo method has been successfully used in predicting the average acquired charge number of arbitrarily shaped particles, as well as the charge distribution on the spherical particles. Moreover, researchers also developed different numerical techniques to analyze the ion density distribution and particle charging process in unipolar chargers. While the previous simulations were largely based on chargers of coaxial configuration, unipolar chargers with complex geometries were also numerically modelled and investigated in recent studies. Numerical predictions on charging efficiencies showed good agreement with the experimental values, and the models are thus able to facilitate the design of unipolar chargers for airborne particles.

Towards the recent developments on the design of unipolar chargers, in order to increase extrinsic charging efficiencies and minimize the electrostatic loss of charged particles, it is concluded that structural designs such as separating corona and mixing chambers have been used, and novel discharging electrodes have been developed and evaluated, specific flow rates and sheath air have been adopted. Furthermore, with the assistant of charged particle measurement techniques such as traditional trajectory analysis and Millikan cell as well as online measurement techniques based on different mobility analyzers, such as DMA and TDMA systems, the extrinsic charging efficiencies were adopted to evaluate the charging effects, most of which have been proved consistency with theoretical results. With the developed unipolar charger, the measurement accuracy of particle measurement instruments such as DMA, APM, etc. is improved since errors caused by particle loss due to electrostatic dispersion and particle diffusion is eliminated and corrected by sheath air, which also has the function as dilution air to reduce particle concentration and to expand applicable scope.

Despite those remarkable progresses made by researchers in the past decades, some important aspects in the unipolar particle charging still remain undercover:

- Some researchers (Penney and Lynch, 1957; McDonald *et al.*, 1980; Aliat *et al.*, 2008; 2009) once suggested a ‘free electron charging’ mechanism at high Ni-t products, or high temperature ionizations, which have not widely accepted by researchers.
- Ion properties are the key parameters in the calculation of models listed in this paper, however, the values of ion mobility and mass reported in the aerosol charging literature lie within a considerable wide range of values. And large variations may exist between the calculation

results using different ion properties.

- All of the charging models mentioned above were derived on the assumptions that particle are solid sphere or agglomerates with perfect surface. However, airborne particles in nature may exhibit different porosity, chemical composition and surface roughness, which may have great effect on the charging behavior.
- Most of the above-mentioned experiments on this topic were conducted in the air atmosphere under standard conditions, which is definitely inadequate to illustrate the effect of environmental factors on the unipolar charging process, such as different operating temperature, humidity, pressure and gas compositions.

Summing up all the above, further studies regarding the unipolar charging process with more specific values of ion properties, real airborne particles and non-standard operation conditions are still highly needed.

ACKNOWLEDGMENT

The authors wish to acknowledge the support from the National Science Fund for Distinguished Young Scholars (No. 51125025), National Program on Key Basic Research Project (973 Program) (No. 2013CB228504), the National Science and Technology Support Program (No. 2015BAA05B02), Hangzhou Science and Technology Development project (No. 20140533B48).

NOMENCLATURE

Roman

a	particle radius, m
b	distance in Eqs. (8) and (9), m
$\bar{c}$	the mean thermal velocity of the ions, m s^{-1}
C_p	electrical capacitance in Eqs. (17) and (18), F
d_p	particle diameter, m
D_i	ionic diffusion coefficient, equals to Z(k/e)T, m^2 s^{-1}
e	elementary unit of charge, ≈1.602×10^{-19} C
E	electric strength, V m^{-1}
F_i	the force vector per unit mass acting on an ion owing to the presence of charge on the particle in Eqs. (14) and (15), N
f_i	the velocity distribution functions of ions in the neighborhood of the particle in Eqs. (14) and (15)
f_j	the velocity distribution functions of neutral gas molecules in the neighborhood of the particle in Eqs. (14) and (15)
I	current through the limiting sphere, A
J	current density, A m^{-2}
k	Boltzmann constant, 1.3806×10^{-23} J K^{-1}
Kn	Knudsen number, equals to $2\lambda/d_p$
m_i	ion mass, kg
N_p	particle concentration, 1 m^{-3}
$N_{p,n}$	concentration of airborne particles with n elementary charges, 1 m^{-3}
N_i	ion concentration, 1 m^{-3}
$N_{i,\infty}$	ion concentration at infinity, 1 m^{-3}
$N_i(\delta,q,\theta)$	ion concentration in the limiting sphere as a function of δ, q and θ, in Eq. (13), 1 m^{-3}
N_it	a parameter to describe the operation effect of a charger, equals to mean ion number concentration × aerosol residence time, s m^{-3}
n_p	mean number of charge of airborne particle in Eq. (18)
q	particle charge, C
q_s	saturation charge, equals to $(3\varepsilon_s/(\varepsilon_s + 2))\pi\varepsilon_0 d_p^2 E_0$, C
r	distance from the center of the particle, in Eq. (3), m
S_p	the geometric surface area of particle in Eq. (18), m^2
t	discharging time, s
T	temperature, K
v	equals to $qe/2\pi\varepsilon_0 d_p kT$, the dimensionless particle charge in Eq. (7)
v_i	velocity vectors of ions in Eqs. (14) and (15), m s^{-1}
v_j	velocity vectors of neutral gas molecules in Eqs. (14) and (15), m s^{-1}
V_p	the electric potential of a particle relative to the potential at large distance, V
w	equals to $w = (\varepsilon_s/\varepsilon_s + 2)(Ed_pe/2kT)$ is the dimensionless electric field strength in Eq. (7)
X	the spacial vector in Eqs. (14) and (15)
x	equals to r/a in Eq. (3)
Z	electrical mobility of ions, m^2 $(Vs)^{-1}$

Greek

α	the fraction of all the emerging ions reaches the particle surface
β_i	integral combination coefficients in equation 13, equals to $I/(eN_{i,\infty})$, m^3 s^{-1}
β_n	combination coefficient of ions with airborne particles carrying n elementary charges in Eq. (16)
$\beta_{p;i}$	collision rate coefficient or kernel of ions and particle
λ	mean free path of gas, m
ε_0	vacuum dielectric constant, 8.85×10^{-12} F/m
ε_s	specific dielectric constant, F/m
δ	the limiting-sphere radius, m
$\varphi(\rho)$	the potential of the ion
ϕ_p	non-dimensional surface potential, equals to $eV_p/(kT)$, in Eq. (18)
Γ_i	the appropriate collision operators of ions in equation Eqs. (14) and (15)
Γ_j	the appropriate collision operators of neutral gas molecules in Eqs. (14) and (15)

REFERENCE

Adachi, M., Kousaka, Y. and Okuyama, K. (1985). Unipolar and bipolar diffusion charging of ultrafine aerosol particles. *J. Aerosol Sci.* 16: 109–123.

Adachi, M., Kusumi, M. and Tsukui, S. (2004). Ion-induced nucleation in nanoparticle synthesis by ionization

chemical vapor deposition. *Aerosol Sci. Technol.* 38: 496–505.

Adamiak, K. (1997). Particle charging by unipolar ionic bombardment in an AC electric field. *IEEE Trans. Ind. Appl.* 33: 421–426.

Alguacil, F.J. and Alonso, M. (2006). Multiple charging of ultrafine particles in a corona charger. *J. Aerosol Sci.* 37: 875–884.

Aliat, A., Tsai, C.J., Hung, C.T. and Wu, J.S. (2008). Effect of free electrons on nanoparticle charging in a negative direct current corona charger. *Appl. Phys. Lett.* 93: 154103.

Aliat, A., Hung, C.T., Tsai, C.J. and Wu, J.S. (2009). Implementation of Fuchs' model of ion diffusion charging of nanoparticles considering the electron contribution in dc-corona chargers in high charge densities. *J. Phys. D: Appl. Phys.* 42: 125206.

Alisoy, H.Z., Alisoy, G.T. and Koseoglu, M. (2005). Charging kinetics of spherical dielectric particles in a unipolar corona field. *J. Electrostat.* 63: 1095–1103.

Alisoy, H.Z., Alagoz, B.B. and Alisoy, G.H. (2010). An analysis of corona field charging kinetics for polydisperse aerosol particles by considering concentration and mobility. *J. Phys. D: Appl. Phys.* 43: 365205.

Alisoy, H.Z., Alagoz, S., Alisoy, G.H. and Alagoz, B.B. (2012). A numerical method for the analysis of polydisperse aerosol particles charging in a coaxial electrode system. *J. Electrostat.* 70: 111–116.

Alonso, M. and Alguacil, F.J. (2003). The effect of ion and particle losses in a diffusion charger on reaching a stationary charge distribution. *J. Aerosol Sci.* 34: 1647–1664.

Alonso, M. and Alguacil, F.J. (2007). Penetration of aerosol undergoing combined electrostatic dispersion and diffusion in a cylindrical tube. *J. Aerosol Sci.* 38: 481–493.

Alonso, M., Alguacil, F.J. and Borra, J.P. (2009). A numerical study of the influence of ion-aerosol mixing on unipolar charging in a laminar flow tube. *J. Aerosol Sci.* 40: 693–706.

Alonso, M. and Huang, C.H. (2015). High-efficiency electrical charger for nanoparticles. *J. Nanopart. Res.* 17: 1–8.

Aurela, M., Saarikoski, S., Niemi, J.V., Canonaco, F., Prevot, A.S.H., Frey, A., Carbone, S., Kousa, A. and Hillamo, R. (2015). Chemical and source characterization of submicron particles at residential and traffic sites in the Helsinki Metropolitan area, Finland. *Aerosol Air Qual. Res.* 15: 1213–1226.

Büscher, P., Schmidt-Ott, A. and Wiedensohler, A. (1994). Performance of a unipolar "square wave" diffusion charger with variable nt-product. *J. Aerosol Sci.* 25: 651–663.

Biskos, G., Mastorakos, E. and Collings, N. (2004). Monte-Carlo simulation of unipolar diffusion charging for spherical and non-spherical particles. *J. Aerosol Sci.* 35: 707–730.

Biskos, G., Reavell, K. and Collings, N. (2005). Unipolar diffusion charging of aerosol particles in the transition regime. *J. Aerosol Sci.* 36: 247–265.

Boisdron, Y. and Brock, J.R. (1970). On the stochastic nature of the acquisition of electrical charge and radioactivity by aerosol particles. *Atmos. Environ.* 4: 35–50.

Bricard, J. (1949). L'equilibre ionique de la basse atmosphere. *J. Geophys. Res*. 54: 39–52.

Chang, J.S. (1981). Theory of diffusion charging of arbitrarily shaped conductive aerosol particles by unipolar ions. *J. Aerosol Sci.* 12: 19–26.

Chen, D.R. and Pui, D.Y.H. (1999). A high efficiency, high throughput unipolar aerosol charger for nanoparticles. *J. Nanopart. Res.* 1: 115–126.

Cheruiyot, N.K., Lee, W.J., Mwangi, J.K., Wang, L.C., Lin, N.H., Lin, Y.C., Cao, J.J., Zhang, R.J. and Chang-Chien, G.P. (2015). An overview: Polycyclic aromatic hydrocarbon emissions from the stationary and mobile sources and in the ambient air. *Aerosol Air Qual. Res.* 15: 2730–2762.

Chien, C.L., Tsai, C.J., Chen, H.L., Lin, G.Y. and Wu, J.S. (2011). Modeling and validation of nanoparticle charging efficiency of a single-wire corona unipolar charger. *Aerosol Sci. Technol.* 45: 1468–1479.

Chien, C.L. and Tsai, C.J. (2013). Improvement of the nanoparticle charging efficiency of a single-wire corona unipolar charger by using radial sheath airflow: Numerical study. *Aerosol Sci. Technol.* 47: 417–426.

Choi, J., Kim, H.J., Kim, Y.J., Kim, S.S. and Jung, J.H. (2016). Novel electrostatic precipitator using unipolar soft X-ray charger for removing fine particles: Application to a dry de-NO_x process. *J. Hazard. Mater.* 303: 48–54.

Clack, H.L. (2015). Simultaneous removal of particulate matter and gas-phase pollutants within electrostatic precipitators: Coupled in-flight and wall-bounded adsorption. *Aerosol Air Qual. Res.* 15: 2445–2455.

Domat, M., Kruis, F.E. and Fernandez-Diaz, J.M. (2014a). Determination of the relevant charging parameters for the modeling of unipolar chargers. *J. Aerosol Sci.* 71: 16–28.

Domat, M., Kruis, F.E. and Fernandez-Diaz, J.M. (2014b). Investigations of the effect of electrode gap on the performance of a corona charger having separated corona and charging zones. *J. Aerosol Sci.* 68: 1–13.

Filippov, A.V. (1993). Charging of aerosol in the transition regime. *J. Aerosol Sci.* 24: 423–436.

Frank, G.P., Cederfelt, S.I. and Martinsson, B.G. (2004). Characterisation of a unipolar charger for droplet aerosols of 0.1-20 μm in diameter. *J. Aerosol Sci.* 35: 117–134.

Fuchs, N., Petrjanoff, I. and Rotzeig, B. (1936). On the rate of charging of droplets by an ionic current. *Trans. Faraday Soc.* 32: 1131–1138.

Fuchs, N.A. (1947). On the Charging of Particles in Atmospheric Aerosols. *Izv. Akad. Nauk SSSR Ser. Geogr. Geofiz.* 11: 341–348.

Fuchs, N.A. (1963). On the stationary charge distribution on aerosol particles in a bipolar ionic atmosphere. *Geofis. Pura Appl.* 56: 185–193.

Gentry, J. and Brock, J.R. (1967). Unipolar diffusion charging of small aerosol particles. *J. Chem. Phys.* 47:

64–69.
Gentry, J.W. (1972). Charging of aerosol by unipolar diffusion of ions. *J. Aerosol Sci.* 3: 65–76.
Gopalakrishnan, R., Thajudeen, T., Ouyang, H. and Hogan, C.J. (2013). The unipolar diffusion charging of arbitrary shaped aerosol particles. *J. Aerosol Sci.* 64: 60–80.
Guo, B.Y., Yang, S.Y., Xing, M., Dong, K.J., Yu, A.B. and Guo, J. (2013). Toward the development of an integrated multiscale model for electrostatic precipitation. *Ind. Eng. Chem. Res.* 52: 11282–11293.
Han, B., Shimada, M., Choi, M. and Okuyama, K. (2003). Unipolar charging of nanosized aerosol particles using soft X-ray photoionization. *Aerosol Sci. Technol.* 37: 330–341.
Han, B., Kim, H.J., Kim, Y.J. and Sioutas, C. (2008). Unipolar charging of fine and ultra-fine particles using carbon fiber ionizers. *Aerosol Sci. Technol.* 42: 793–800.
Hernandez-Sierra, A., Alguacil, F.J. and Alonso, M. (2003). Unipolar charging of nanometer aerosol particles in a corona ionizer. *J. Aerosol Sci.* 34: 733–745.
Hewitt, G.W. (1957). The charging of small particles for electrostatic precipitation. *Trans. Am. Inst. Electr. Eng. Part 1* 76: 300–306.
Hontañón, E. and Kruis, F.E. (2008). Single charging of nanoparticles by UV photoionization at high flow rates. *Aerosol Sci. Technol.* 42: 310–323.
Huang, C.H. and Alonso, M. (2011). Nanoparticle electrostatic loss within corona needle charger during particle-charging process. *J. Nanopart. Res.* 13: 175–184.
Huang, C.H. and Alonso, M. (2012). Influence of particle location on the number of charges per charged nanoparticle at the outlet of a needle charger. *J. Air Waste Manage. Assoc.* 62: 87–91.
Huang, D.D., Seinfeld, J.H. and Marlow, W.H. (1990). BGK equation solution of coagulation for large knudsen number aerosols with a singular attractive contact potential. *J. Colloid Interface Sci.* 140: 258–276.
Intra, P. and Tippayawong, N. (2009). Progress in Unipolar corona discharger designs for airborne particle charging: A literature review. *J. Electrostat.* 67: 605–615.
Intra, P. and Tippayawong, N. (2011). An overview of unipolar charger developments for nanoparticle charging. *Aerosol Air Qual. Res.* 11: 187–209.
Intra, P. (2012). Corona discharge in a cylindrical triode charger for unipolar diffusion aerosol charging. *J. Electrostat.* 70: 136–143.
Kim, D., Kim, Y., Kwon, Y. and Park, K. (2011). Evaluation of a Soft X-Ray unipolar charger for charging nanoparticles. *J. Nanopart. Res.* 13: 579–585.
Kim, J.H., Yoo, H.J., Hwang, Y.S. and Kim, H.G. (2012). Removal of particulate matter in a tubular wet electrostatic precipitator using a water collection electrode. *Sci. World J.* 2012: 532354.
Kim, K.H., Kabir, E. and Kabir, S. (2015). A review on the human health impact of airborne particulate matter. *Environ. Int.* 74: 136–143.
Kim, K.B. and Yoon, B.J. (1997). Field Charging of spherical particles in linear electric field. *J. Colloid Interface Sci.* 186: 209–211.
Kimoto, S., Saiki, K., Kanamaru, M. and Adachi, M. (2010). A small mixing-type unipolar charger (SMUC) for Nanoparticles. *Aerosol Sci. Technol.* 44: 872–880.
Kirsch, A.A. and Zagnit'Ko, A.V. (1981). Diffusion charging of submicrometer aerosol particles by unipolar ions. *J. Colloid Interface Sci.* 80: 111–117.
Kirsch, A.A. and Zagnit'Ko, A.V. (1990). Field charging of fine aerosol-particles by unipolar ions. *Aerosol Sci. Technol.* 12: 465–470.
Koseoglu, M. and Alisoy, H.Z. (2011). The analysis of the charge on a cylindrical dielectric particle in unipolar corona field. *J. Electrostat.* 69: 176–179.
Kulkarni, P., Baron, P.A. and Willeke, K. (2011). *Aerosol Measurement: Principles, Techniques, and Applications*. John Wiley & Sons, New York.
Kwon, S.B., Fujimoto, T., Kuga, Y., Sakurai, H. and Seto, T. (2005). Characteristics of aerosol charge distribution by surface-discharge microplasma aerosol charger (SMAC). *Aerosol Sci. Technol.* 39: 987–1001.
Kwon, S.B., Sakurai, H. and Seto, T. (2007). Unipolar charging of nanoparticles by the surface-discharge microplasma aerosol charger (SMAC). *J. Nanopart. Res.* 9: 621–630.
Lackowski, M. (2001). Unipolar charging of aerosol particles in alternating electric field. *J. Electrostat.* 51: 225–231.
Laframboise, J. and Chang, J.S. (1977). Theory of charge deposition on charged aerosol particles of arbitrary shape. *J. Aerosol Sci.* 8: 331–338.
Lancereau, Q., Roux, J.M. and Achard, J.L. (2013). Influence of secondary flows on the collection efficiency of a cylindrical electrostatic precipitator. *J. Aerosol Sci.* 63: 146–160.
Lawless, P.A. (1996). Particle charging bounds, symmetry relations, and an analytic charging rate model for the continuum regime. *J. Aerosol Sci.* 27: 191–215.
Li, L. and Chen, D.R. (2011a). Aerosol charging using pen-type UV lamps. *Aerosol Air Qual. Res.* 11: 791–801.
Li, L. and Chen, D.R. (2011b). Performance study of a DC-corona-based particle charger for charge conditioning. *J. Aerosol Sci.* 42: 87–99.
Li, Q., Jiang, J.K., Duan, L., Deng, J.G., Jiang, L., Li, Z. and Hao, J.M. (2015). Improving the removal efficiency of elemental mercury by pre-existing aerosol particles in double dielectric barrier discharge treatments. *Aerosol Air Qual. Res.* 15: 1506–1513.
Liang, B., Ge, Y.S., Tan, J.W., Han, X.K., Gao, L.P., Hao, L.J., Ye, W.T. and Dai, P.P. (2013). Comparison of PM emissions from a gasoline direct injected (GDI) vehicle and a port fuel injected (PFI) vehicle measured by electrical low pressure impactor (ELPI) with two fuels: Gasoline and M15 methanol gasoline. *J. Aerosol Sci.* 57: 22–31.
Liu, B. and Kapadia, A. (1978). Combined field and diffusion charging of aerosol particles in the continuum regime. *J. Aerosol Sci.* 9: 227–242.
Liu, B.Y.H., Whitby, K.T. and Yu, H.H.S. (1967a). Diffusion charging of aerosol particles at low pressures. *J. Appl. Phys.* 38: 1592–1597.
Liu, B.Y.H., Whitby, K.T. and Yu, H.H.S. (1967b). On the

theory of charging of aerosol particles by unipolar ions in the absence of an applied electric field. *J. Colloid Interface Sci.* 23: 367–378.

Liu, B.Y.H. and Yeh, H.C. (1968). On theory of charging of aerosol particles in an electric field. *J. Appl. Phys.* 39: 1396.

Long, Z.W. and Yao, Q.A. (2010). Evaluation of various particle charging models for simulating particle dynamics in electrostatic precipitators. *J. Aerosol Sci.* 41: 702–718.

Long, Z.W. and Yao, Q. (2012). Numerical simulation of the flow and the collection mechanism inside a scale hybrid particulate collector. *Powder Technol.* 215–216: 26–37.

Luond, F. and Schlatter, J. (2013). Improved monodispersity of size selected aerosol particles with a new charging and selection scheme for tandem DMA setup. *J. Aerosol Sci.* 62: 40–55.

Lushnikov, A.A. and Kulmala, M. (2005). A kinetic theory of particle charging in the free-molecule regime. *J. Aerosol Sci.* 36: 1069–1088.

Malaguti, A., Mircea, M., La Torretta, T.M.G., Telloli, C., Petralia, E., Stracquadanio, M. and Berico, M. (2015). Chemical composition of fine and coarse aerosol particles in the central mediterranean area during dust and non-dust conditions. *Aerosol Air Qual. Res.* 15: 410–425.

Manirakiza, E., Seto, T., Osone, S., Fukumori, K. and Otani, Y. (2012). high-efficiency unipolar charger for sub-10 nm aerosol particles using surface-discharge microplasma with a voltage of sinc function. *Aerosol Sci. Technol.* 47: 60–68.

Marjamaki, M., Keskinen, J., Chen, D.R. and Pui, D.Y.H. (2000). Performance evaluation of the electrical low-pressure impactor (ELPI). *J. Aerosol Sci.* 31: 249–261.

Marlow, W.H. and Brock, J.R. (1975). Unipolar Charging of Small Aerosol Particles. *J. Colloid Interface Sci.* 50: 32–38.

Marquard, A., Kasper, M., Meyer, J. and Kasper, G. (2005). Nanoparticle charging efficiencies and related charging conditions in a wire-tube ESP at DC energization. *J. Electrostat.* 63: 693–698.

Marquard, A. (2007). Unipolar field and diffusion charging in the transition regime—Part I: A 2-D limiting-sphere model. *Aerosol Sci. Technol.* 41: 597–610.

McDonald, J.R., Anderson, M.H., Mosley, R.B. and Sparks, L.E. (1980). charge measurements on individual particles exiting laboratory precipitators with positive and negative corona at various temperatures. *J. Appl. Phys.* 51: 3632.

Mohnen, V.A. (1976). Formation, Nature, and Mobility of Ions of Atmospheric Importance, In *Electrical Processes in Atmospheres*, Dolezalek, H., Reiter, R. and Landsberg, H. (Eds.), Steinkopff, pp. 1–17.

Murphy, A.T., Adler, F.T. and Penney, G.W. (1959). A theoretical analysis of the effects of an electric field on the charging of fine particles. *Trans. Am. Inst. Electr. Eng. Part 1* 78: 318–326.

Natanson, G.L. (1960). On the theory of the charging of a microscopic aerosol particles as a result of capture of gas ions. *Sov. Phys. Tech. Phys.* 5: 538–551.

Oh, H., Park, H. and Kim, S. (2004). Effects of particle shape on the unipolar diffusion charging of nonspherical particles. *Aerosol Sci. Technol.* 38: 1045–1053.

Park, J., Kim, C., Jeong, J., Lee, S.G. and Hwang, J. (2011a). Design and evaluation of a unipolar aerosol charger to generate highly charged micron-sized aerosol particles. *J. Electrostat.* 69: 126–132.

Park, J.H., Yoon, K.Y. and Hwang, J. (2011b). Removal of submicron particles using a carbon fiber ionizer-assisted medium air filter in a heating, ventilation, and air-conditioning (HVAC) system. *Build. Environ.* 46: 1699–1708.

Park, K.T., Park, D., Lee, S.G. and Hwang, J. (2009). Design and performance test of a multi-channel diffusion charger for real-time measurements of submicron aerosol particles having a unimodal log-normal size distribution *J. Aerosol Sci.* 40: 858–867.

Pauthenier and Moreau-Hanot, M. (1932). Spherical particle charges in an ionized field. *J. Phys. Radium.* 3: 590–613.

Penney, G.W. and Lynch, R.D. (1957). Measurements of charge imparted to fine particles by a corona discharge. *Trans. Am. Inst. Electr. Eng. Part 1* 76: 294–299.

Pui, D.Y.H., Fruin, S. and Mcmurry, P.H. (1988). Unipolar diffusion charging of ultrafine aerosols. *Aerosol Sci. Technol.* 8: 173–187.

Qi, C., Chen, D.R. and Pui, D.Y.H. (2007). Experimental study of a new corona-based unipolar aerosol charger. *J. Aerosol Sci.* 38: 775–792.

Qi, C., Chen, D.R. and Greenberg, P. (2008). Performance study of a unipolar aerosol mini-charger for a personal nanoparticle sizer. *J. Aerosol Sci.* 39: 450–459.

Qi, C., Asbach, C., Shin, W.G., Fissan, H. and Pui, D.Y.H. (2009). The effect of particle pre-existing charge on unipolar charging and its implication on electrical aerosol measurements. *Aerosol Sci. Technol.* 43: 232–240.

Qi, C.L. and Kulkarni, P. (2012). Unipolar charging based, hand-held xmobility spectrometer for aerosol size distribution measurement. *J. Aerosol Sci.* 49: 32–47.

Reischl, G.P., Mäkelä, J.M., Karch, R. and Necid, J. (1996). bipolar charging of ultrafine particles in the size range below 10 nm. *J. Aerosol Sci.* 27: 931–949.

Romay, F.J. and Pui, D.Y.H. (1992). On the combination coefficient of positive ions with ultrafine neutral particles in the transition and free-molecule regimes. *Aerosol Sci. Technol.* 17: 134–147.

Sambudi, N.S., Choi, H.J., Lee, M.H. and Cho, K. (2016). Capture of ultrafine particles using a film-type electret filter with a unipolar charger. *Aerosol Air Qual. Res., in Press.*

Samuila, A., Mihailescu, M. and Dascalescu, L. (1998). Unipolar charging of insulating spheres in rectified AC electric fields. *IEEE Trans. Ind. Appl.* 34: 726–731.

Seto, T., Orii, T., Hirasawa, M., Aya, N. and Shimura, H. (2003). Ion beam charging of silicon nanoparticles in helium background gas: Design of the ion beam aerosol charger. *Rev. Sci. Instrum.* 74: 3027–3030.

Seto, T., Orii, T., Sakurai, H., Hirasawa, M. and Kwon, S.B. (2005). Ion beam charging of aerosol nanoparticles.

Aerosol Sci. Technol. 39: 750–759.

Shimada, M., Han, B., Okuyama, K. and Otani, Y. (2002). Bipolar charging of aerosol nanoparticles by a soft X-ray photoionizer. *J. Chem. Eng. Jpn.* 35: 786–793.

Shin, W.G., Qi, C., Wang, J., Fissan, H. and Pui, D.Y.H. (2009). The effect of dielectric constant of materials on unipolar diffusion charging of nanoparticles. *J. Aerosol Sci.* 40: 463–468.

Shin, W.G., Wang, J., Mertler, M., Sachweh, B., Fissan, H. and Pui, D.Y.H. (2010). The effect of particle morphology on unipolar diffusion charging of nanoparticle agglomerates in the transition regime. *J. Aerosol Sci.* 41: 975–986.

Smith, W.B. and McDonald, J.R. (1975). Calculation of the charging rate of fine particles by unipolar ions. *J. Air Pollut. Control Assoc.* 25: 168–172.

Tsai, C.J., Chen, S.C., Chen, H.L., Chein, H.M., Wu, C.H. and Chen, T.M. (2008). Study of a nanoparticle charger containing multiple discharging wires in a tube. *Sep. Sci. Technol.* 43: 3476–3493.

Tsai, C.J., Lin, G.Y., Chen, H.L., Huang, C.H. and Alonso, M. (2010). Enhancement of Extrinsic charging efficiency of a nanoparticle charger with multiple discharging wires. *Aerosol Sci. Technol.* 44: 807–816.

Vivas, M.M., Hontañón, E. and Schmidt-Ott, A. (2008a). Design and evaluation of a low-level radioactive aerosol charger based on ^{241}Am *J. Aerosol Sci.* 39: 191–210.

Vivas, M.M., Hontanon, E. and Schmidt-Ott, A. (2008b). Reducing multiple charging of submicron aerosols in a corona diffusion charger. *Aerosol Sci. Technol.* 42: 97–109.

White, H.J. (1951). Particle charging in electrostatic precipitation. *Trans. Am. Inst. Electr. Eng.* 70: 1186–1191.

Whitby, K.T. (1961). Generator for producing high concentrations of small ions. *Rev. Sci. Instrum.*32: 1351–1355.

Zevenhoven, C.A.P. (1999). Uni-polar field charging of particles: Effects of particle conductivity and rotation. *J. Electrostat.* 46: 1–12.

Received for review, July 19, 2016
Revised, October 28, 2016
Accepted, October 29, 2016